Nanoscale Res Lett (2010) 5:1320–1323
DOI 10.1007/s11671-010-9645-7

NANO EXPRESS

Multilayers of InGaAs Nanostructures Grown on GaAs(210) Substrates

Zhiming M. Wang · Yanze Z. Xie · Vasyl P. Kunets · Vitaliy G. Dorogan · Yuriy I. Mazur · Gregory J. Salamo

Received: 4 March 2010 / Accepted: 10 May 2010 / Published online: 27 May 2010

Abstract Multilayers of InGaAs nanostructures are grown on GaAs(210) by molecular beam epitaxy. With reducing the thickness of GaAs interlayer spacer, a transition from InGaAs quantum dashes to arrow-like nanostructures is observed by atomic force microscopy. Photoluminescence measurements reveal all the samples of different spacers with good optical properties. By adjusting the InGaAs coverage, both one-dimensional and two-dimensional lateral ordering of InGaAs/GaAs(210) nanostructures are achieved.

Keywords Molecular beam epitaxy · InGaAs nanostructures · GaAs(210) · Lateral ordering

On GaAs(100), the extensively investigated surface orientation, the InGaAs growth proceeds in a fashion of two-dimensional (2D) layering plus nanoscale 3D islanding, as driven by strain elastic relaxation due to sufficient lattice mismatch. The resulted 3D islands buried in the GaAs matrix, so-called quantum dots (QDs), have attracted a lot of attentions in the field of the compound semiconductor research in the last 15 years, for their rich spectrum of optoelectronic applications [1–4]. On the other hand, on GaAs(110), another important low index surface orientation, the InGaAs growth proceeds in a layer-by-layer 2D mode without introducing 3D islands [5, 6]. The accumulating strain is expected to be relaxed in a later stage through introducing misfit dislocations. Since (110) is the natural cleaved face of GaAs substrates, the unique growth mechanism leads to cleaved-edge overgrowth of aligned InGaAs QDs through incorporated Al content into the underlying growth base [7, 8].

The InGaAs growth on GaAs high-index substrates orientated between (100) and (110) is still a mystery. On the other hand, other high-index surfaces, especially GaAs(n11), have received significant attention and hosted wide range of InGaAs nanostructures with distinguished functions. For example, InGaAs quantum wires are observed on GaAs(311)A and a unique growth mode is revealed, starting from 2D, through 1D, and finally leading to 3D [9]. Most recently, a remarkable achievement is the ability to tune both vertical and lateral alignments of QDs in InGaAs multilayers on GaAs(n11)B [10].

GaAs(210) is a plane located in between (100) and (110), 26.6° away from (100) and 18.4° away from (110). In this letter, we reveal the growth phenomena of InGaAs multilayers on GaAs(210) and demonstrate lateral ordered arrays of both quantum dashes and quantum wires.

All samples presented in this study were grown using solid source Molecular Beam Epitaxy (MBE) 32P Riber system. After growth of 0.5-μm-thick GaAs buffer layer at 580°C with a growth rate of 1 monolayer per second (ML/s) under a constant As beam equivalent pressure of 1×10^{-5} Torr, 15.5 periods multilayered $In_{0.4}Ga_{0.6}As$/GaAs structures of different GaAs spacer layer thicknesses or of different $In_{0.4}Ga_{0.6}As$ coverages were grown. Three samples of different spacers at 120, 70, and 50 ML respectively have the same $In_{0.4}Ga_{0.6}As$ coverage of 7 ML. One additional sample of 70 ML spacer has the $In_{0.4}Ga_{0.6}As$ coverage of 5.7 ML. The growth of $In_{0.4}Ga_{0.6}As$ layer was performed at 540°C and As beam equivalent pressure of 4.4×10^{-6} Torr. After growth of

Zh. M. Wang · Y. Z. Xie · Vas. P. Kunets · V. G. Dorogan · Yu. I. Mazur (✉) · G. J. Salamo
Arkansas Institute for Nanoscale Materials Science and Engineering, University of Arkanssas, Fayetteville, AR 72701, USA
e-mail: ymazur@uark.edu

first 5 ML of GaAs spacer at 540°C, the temperature of growth was rapidly increased up to 580°C, and As beam equivalent pressure was turned back to 1×10^{-5} Torr. The quality of growth and growth rates were monitored by RHEED. All growths were ended by $In_{0.4}Ga_{0.6}As$ layer for following atomic force microscopy (AFM) studies. For optical properties of the samples, the photoluminescence (PL) measurements were performed in a variable temperature 10–300 K closed-cycle helium cryostat. The 532-nm line from a Nd:YAG (yttrium aluminum garnet) laser was used for continuous-wave (CW) PL excitation. The laser spot diameter was about 20 μm and the optical excitation power was in the range of 10^{-6}–10^{2} mW. The PL signal from the sample was dispersed by a 0.5-m single-grating monochromator and detected by liquid nitrogen (LN)-cooled InGaAs photodiode detector array.

Figure 1 is a morphology overview of the three samples with different spacers in thickness. Figure 1a is an AFM image of the sample of 120 ML spacer. The surface is characterized as quantum dashes elongated along [-100] direction. With reducing the GaAs spacer to 70 ML, the quantum dashes are getting shorter, as shown in Fig. 1b. Further reducing the spacer thickness to 50 ML, the InGaAs nanostructures become arrow like, as shown in Fig. 1c.

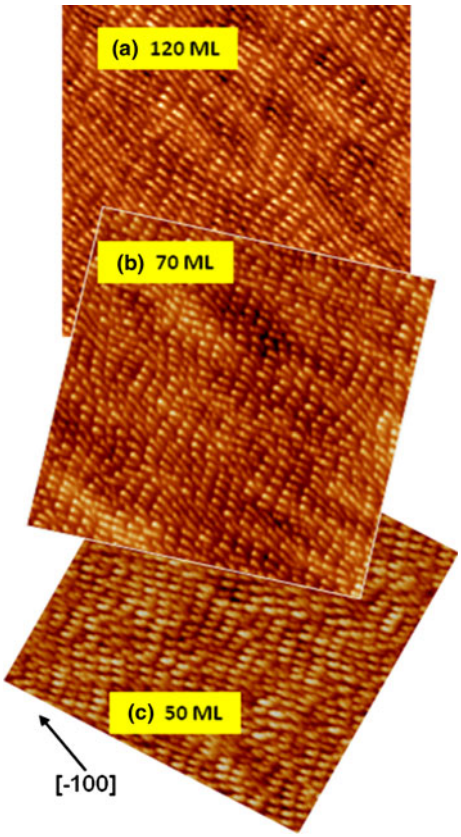

Fig. 1 AFM images of (210) surface of InGaAs multilayers spaced by GaAs in 120 ML (**a**), 70 ML (**b**), and 50 ML (**c**). Scanning size: 5 × 5 μm

Please notice, PL spectra in Fig. 2 demonstrate all the samples with excellent optical properties, similar to previous data on GaAs(100) and other indexed substrates [11, 12]. According to previous reports, the narrow peaks around 960 nm and the broad peaks in the range of 1100–1200 nm can be respectively identified as from the 15 layers of buried InGaAs nanostructures and the surface InGaAs nanostructures exposed for AFM imaging. With reducing the thickness of GaAs spacers, the buried InGaAs nanostructures are getting closer to the exposed surface InGaAs nanostructures, and the optically excited carriers are then getting easier to transfer from the buried layers to the surface. The mechanism of carrier transfer explains the variation of the relative intensity of two PL peeks from different samples. Such a hybrid of surface and buried nanostructures has been proposed for its potential application in biological biosensing [11, 12].

The AFM data in Fig. 1 suggest a structural coupling and the PL data in Fig. 2 indicate an electronic coupling between subsequent InGaAs layers. Since the growth mechanism has been well documented [13, 14], vertical alignments of InGaAs nanostructures as a result of strain field interaction among subsequent layers are expected. With reducing the spacer thickness, more strain fields transmitted to the following layer; therefore, the growth proceeds in a more efficient approach to relax the accumulating strain. As the result, the quantum dashes become shorter and a transition to arrow-like nanostructures is observed.

The build-up strain energy can be more efficiently tuned by adjusting the InGaAs coverage. Figure 3 shows AFM images in two different scales for the sample with the InGaAs coverage of 5.7 ML, while keeping the same spacer thickness of 70 ML as in Fig. 1b. Figure 3a clearly demonstrates that the InGaAs nanostructures are better

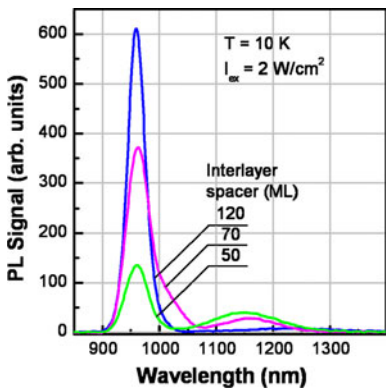

Fig. 2 PL spectra of InGaAs/GaAs(210) multilayers with different spacers in thickness

described as quantum wires, even though there is frequent height modulation among the wires observed. Comparing the AFM images of two samples with different InGaAs coverage at the same scale, it shows that the lateral spacing between quantum wires in Fig. 3b is much smaller than that of quantum dashes in Fig. 1b.

To quantitatively compare two samples' surface morphologies, the 2D autocorrelation functions are calculated from AFM images (2.5 × 2.5 μm) for both samples and shown in Fig. 4 [15]. The sample of 7 ML coverage has nice 2D lateral ordering as revealed in Fig. 4a. The separation between quantum dashes along [-100] direction is 269.6 nm on average and the nearest distance between quantum dashes is 128.3 nm on average. The nearest direction is about 60 ^{o} away from [-100]. The surface of the sample with 5.7 ML coverage is characterized with 1D lateral ordering, only with weak intensity modulation along [-100], as shown in Fig. 4b. The quantum wires observed are much denser, and their separation is 84.5 nm on average. The height modulation along wires is weak but still resolved with a periodicity of about 186.3 nm. The dramatic change of the nanostructure configuration and lateral ordering due to the change of InGaAs coverage is consistent with the observation in Fig. 1 as the function of spacer thickness. By reducing the InGaAs coverage from 7 to 5.7 ML, the build-up strain is significantly reduced and therefore the quantum dashes are significantly elongated toward wire-like structures.

In conclusion, the nanostructure evolution of InGaAs/GaAs multilayers along (210) is investigated. 2D-ordered quantum dashes and uniformly spaced quantum wires are observed. The results are explained in terms of strain-driven mechanism with considering the amount of strain build-up. Such a report of InGaAs nanostructures on a surface index between (100) and (110) could help to achieve a comprehensive understanding of strain-driven growth in general.

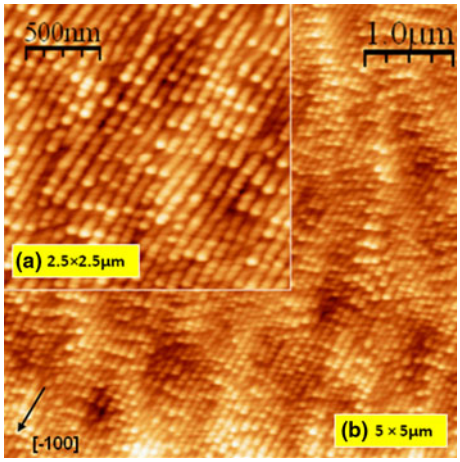

Fig. 3 AFM images of (210) surface with InGaAs coverage of 5.7 ML. Scanning size (**a**) 2.5 × 2.5 μm; (**b**) 5 × 5 μm

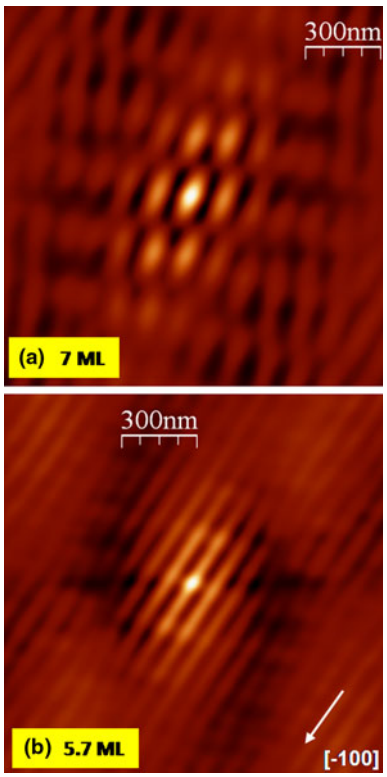

Fig. 4 2D images of autocorrelation functions calculated from AFM images for samples as shown in Fig. 1a and Fig. 3, with InGaAs coverage of 7 ML (**a**) and 5.7 ML (**b**), respectively

References

1. D. Leonard, M. Krishnamurthy, C.M. Reaves, S.P. Denbaars, P.M. Petroff, Appl. Phys. Lett. **63**, 3203 (1993)
2. D. Bimberg, M. Grundmann, N.N. Ledentsov, *Quantum Dot Heterostructures* (Wiley, Chichester, 1999)
3. S.-S. Li, J.-B. Xia, J.-L. Liu, F.-H. Yang, Z.-C. Niu, S.-L. Feng, H.-Z. Zheng, J. Appl. Phys. **90**, 6151 (2001)
4. J. Pakarinen, V. Polojärvi, A. Aho, P. Laukkanen, C.S. Peng, A. Schramm, A. Tukiainen, M. Pessa, Appl. Phys. Lett. **94**, 072105 (2009)
5. B.A. Joyce, T.S. Jones, J.G. Belk, J. Vac. Sci. Technol. B **16**, 2373 (1998)
6. D. Wasserman, S.A. Lyon, M. Hadjipanayi, A. Maciel, J.F. Ryan, Appl. Phys. Lett. **83**, 5050 (2003)
7. D. Wasserman, S.A. Lyon, Appl. Phys. Lett. **85**, 5352 (2004)
8. E. Uccelli, M. Bichler, S. Nuernberger, G. Abstreiter, A. Fontcuberta i Morral, Nanotechnology **19**, 045303 (2008)
9. H. Wen, Z.M. Wang, G.J. Salamo, Appl. Phys. Lett. **84**, 1756 (2004)

10. M. Schmidbauer, S. Seydmohamadi, D. Grigoriev, Zh.H.M. Wang, Yu.I. Mazur, P. Schafer, M. Hanke, R. Kohler, G.J. Salamo, Phys. Rev. Lett. **96**, 066108 (2006)
11. B.L. Liang, Zh.H.M. Wang, Yu.I. Mazur, G.J. Salamo, E.A. DeCuir Jr., M.O. Manasreh, Appl. Phys. Lett. **89**, 043125 (2006)
12. B.L. Liang, Zh.H.M. Wang, Yu.I. Mazur, S.H. Seydmohamadi, M.E. Ware, G.J. Salamo, Optics Express **15**, 8157 (2007)
13. Q. Xie, A. Madhukar, P. Chen, N.P. Kobayashi, Phys. Rev. Lett. **75**, 2542 (1995)
14. G.S. Solomon, J.A. Trezza, A.F. Marshall, J.J.S. Harris, Phys. Rev. Lett. **76**, 952 (1996)
15. Z.M. Wang, J.L. Shultz, G.J. Salamo, Appl. Phys. Lett. **83**, 1749 (2003)